Molecular dynamics simulation of synchronization in driven particles

Tiare Guerrero* and Danielle McDermott†
Department of Physics, Pacific University, Forest Grove, OR 97116
(Dated: January 30, 2021)

Synchronization plays a key role in many physical processes. We discuss a simple numerical model of synchronized particles using molecular dynamics simulations for particles moving through a viscous liquid. Modeling synchronization with simulations and table-top experiments can provide insight to complex behaviors in the natural world. We drive particles across a washboard potential energy landscape, a common technique to isolate complex synchronized patterns in both simulations and experiments. Our results show a variety of synchronization effects in single and multi-particle systems, which we characterize with plots of particle velocity as a function of applied driving force, and phase diagrams of position versus velocity.

I. INTRODUCTION

Synchronization is a universal phenomena in which individual oscillators adjust frequency due to external stimulus [1]. Many everyday systems exhibit in-phase coupled oscillations such as the flickering patterns of candle flames mediated by temperature fluctuations [3], vibrations of singing wineglasses interacting through sound waves [4], and metronomes vibrating through a supporting platform [5]. Biological systems benefit from cooperative synchronization – birds coordinate wing flaps to optimize energy use during flight [6], frogs alternate croaking patterns [7], humans clap in time with music [8] and at a cellular level, neurons simultaneously fire in cardiac muscle [9] and brain tissue [10]. External forcing can cause or regulate synchronization. For instance, an electrical pacemaker pulses to regulate a heart beat, and a flashing light can modify the pattern of flashing fireflies .

A particular form of synchronization is phase-locking or mode-locking, which first appeared in the scientific literature with Huygens' 1665 experiments on the motions of two wall-mounted pendulum clocks. Huygens demonstrated the tendency of the pendula to swing in time, even when started out of phase, due to interactions through the wall [2]. Dynamical systems exhibit phase-locking when oscillators with different rhythms adjust to a frequency ratio or mode of an integer number [12]. Synchronization is often studied with simple computational models and can be visualized with phase plots or Lissajous figures. In phase space a mode-locked system is confined to a closed loop in a parametric space showing the relationship between two periodic functions with patterns determined by the mode, first reported in 1857 [13] and easily generated with a computer code or oscilloscope [14]. It should be noted that the term phase has two scientific meanings, "oscillation phase" and "phase space" Oscillation phase ϕ_0 is the constant portion of the argument in a periodic function $\sin(\omega t + \phi_0)$ while phase space refers to plots of velocity versus position (such as v_y vs. y) that are used to characterize oscillating systems.

Complex dynamics can be studied with colloid particles with experiments and simulation. In typical experiments colloids are spheres of plastic suspended in highly de-ionized water or silica in suspended in organic solvent. Because the spheres are a few microns in size and move at rates of microns per second, the position of a particle can be imaged as a function of time with a traditional optical camera. Individual colloids exhibit Brownian motion, where particles change direction due to collisions with unseen particles comprising the suspending fluid [].

Light is a tool for manipulating the colloidal environment. A single laser beam can be used to create an optical trap, which uses photon radiation pressure to control colloid motions [30]. A circular optical trap is designed with a local energy minimum at its center. A colloid in the beam center is subject to a uniform distribution of photon bombardment, and motions away from the center create a net force due to an uneven distribution of photon collisions on its surface. Depending on the location of the particle in the trap, the radiation pressure either restores colloids toward the local minima or ejects it from the trap. An optically trapped colloid executing Brownian motion is a useful probe of microscopic forces, and has been studied in detail in Ref. [31].

Complex environments can be engineered with light by using diffraction gratings to create a patterned potential energy landscape with one or more laser beams [29]. How a particle moves in an optical landscape can change when subject to external driving forces. Individual particles can perform synchronized motions that lock together particle location and velocity. Experimental studies of the microscopic dynamics colloids performing phase-locked motions produce step-by-step diagrams of particle dynamics useful for understanding synchronization at a single particle level [25].

Here we perform numerical studies on the synchronized dynamics of confined particles driven over a washboard shaped potential energy landscape. We chose this model for its relevance to condensed matter systems and ease of simulation. We describe our molecular dynamics model for a single particle in Section II. We summarize our results including synchronized motion of a single confined particle driven across a periodic landscape in Section III.

*Electronic address: guer9330@pacificu.edu
†Electronic address: mcdermott@pacific.edu

We include exercises for interested students in Section IV. In Section V we describe how our work with colloids applies more broadly to many physical systems such as dusty plasmas, superconducting vortices and Josephson junctions.

II. MOLECULAR DYNAMICS SIMULATION

We use a classical model for studying the dynamics of N interacting particles, using the net force on each particle to calculate its trajectory. Particles are confined in a two-dimensional (2D) simulation of area $A = L \times L$ where $L = 36.5a_0$ where a_0 is a dimensionless unit of length. An individual particle i has position $\vec{r}_i = x_i\hat{x} + y_i\hat{y}$ and velocity $\vec{v}_i = d\vec{r}_i/dt$. The edges of the system are treated with periodic boundary conditions such that a particle leaving the edge of the system is mapped back to a position within the simulation boundaries by the transformation $x_i + L \to x_i$ and $y_i + L \to y_i$. We show a schematic of the system in Fig. 1(a).

We confine the particles using a position dependent potential energy function, called a landscape or substrate. The landscape is modulated in the y-direction with the periodic function

$$U(y) = U_0 \cos\left(N_p \pi y/L\right) \tag{1}$$

where N_p are the number of periods, and U_0 is an adjustable parameter to set the depth of the minima with simulation units of energy $E_0 = 1$. We plot this function in Fig. 1 for $N_p = 3$. In Fig. 1(a) we show the $x-y$ plane with a contour plot of $U(y)$ to illustrate the 2D potential energy landscape, where the maxima are colored red and the minima colored blue. The confining force on a particle i is calculated as $\vec{F}_i^l(\vec{r}_i) = -\nabla U_l(\vec{r}_i)$. In Fig. 1(b) we plot the function $U(y)$ to illustrate how the magnitude $\vec{F}_i^l$ is calculated from particle position y_i.

Particles are subject an external time-dependent driving force $\vec{F}_D(t)$ applied parallel to the y-direction. We model this force as

$$\vec{F}^d(t) = [F^{dc} + F^{ac}\sin(\omega t)]\hat{y}, \tag{2}$$

with modifiable parameters including a constant component F^{dc}, and a time dependent component with amplitude F^{ac} and frequency $\omega = 2\pi f$.

The inertia of small particles is reduced by interactions with fluid particles [15]. In our model we assume colloids are overdamped – i.e. colloids are suspended in a continuous viscous fluid that dissipates energy such that the particles do not accelerate. Energy dissipation from the fluid is modeled with a frictional force on particle with velocity $\vec{v}_i$ as $\vec{F}_i^{drag} = -\eta\vec{v}_i$ with a friction coefficient η proportional to the fluid viscosity. We discuss friction models for spheres moving through fluids in Exercise IV A.

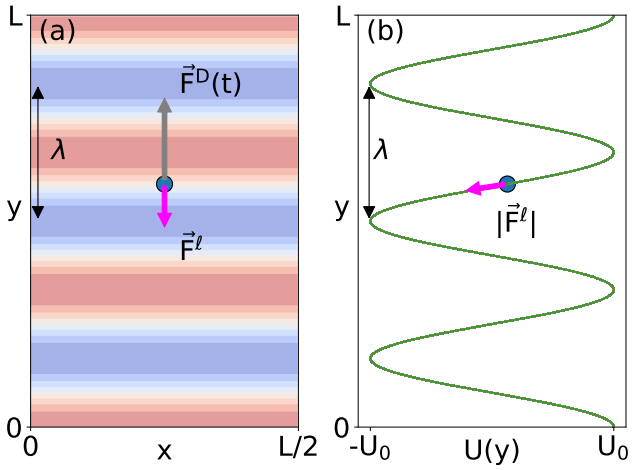

FIG. 1: Schematic of the simulation of a single particle driven across a washboard potential energy landscape. The period of the landscape is $\lambda = L/N_p$, where $N_p = 3$. The force due to the landscape is calculated from the gradient of the potential energy $\vec{F}^l = -\nabla U(\vec{r})$. (a) View of the $x-y$ plane. The time-dependent applied driving force $\vec{F}^d$ is parallel to the y-axis. The landscape is shown with a contour plot, with maxima in the potential energy marked in red and minima marked in blue. A particle is shown in the region between minima and maxima subject to competing forces of the landscape and applied driving force. (b) The potential energy function along the y-axis $U_l(y)$. The particle in (a) is shown at the same $y-$position. The slope of $U_l(y)$ is the magnitude of force $\vec{F}^l$.

Newton's second law for an individual particle is simplified by the assumption $\vec{a}_i$ is zero. The overdamped equation of motion for an isolated particle is

$$\eta\vec{v}_i = \vec{F}_i^l(\vec{r}_i) + \vec{F}^d(t). \tag{3}$$

with $\eta = 1$ in units of v_0/F_0. The equation of motion provides a direct calculation of the velocity of an individual particle from its location $\vec{r}_i$ and the simulation time.

The molecular dynamics simulation is controlled by a $for()$ loop which runs from an initial to maximum integer number of time steps. Each integer time step interval represents a simulation time of Δt simulation units τ. At each time step we evaluate the net force on each particle as a function of its position $\vec{r}_i(t)$ and then integrate the equation of motion to move particles to an updated position. Since the acceleration as zero, the integration of the equation of motion is performed via the Euler method

$$\vec{r}_i(t + \Delta t) = \vec{v}_i(t)\Delta t + \vec{r}_i(t) \tag{4}$$

for a small time step $\Delta t = 0.001\tau$. In Exercise IV C we describe the numerical methods for solving differential equations. The units of the simulated variables are summarized in Table I.

TABLE I: Simulation parameters and units and comparable experimental values [25]. Blanks indicate units, rather than parameters that are not easily represented by a single value.

Quantity	Simulation Unit	Experimental value
length	$a_0 = 1$	$a_0 \sim 1.5\mu m$
energy	$E_0 = 1$	
force	$F_0 = E_0/a_0$	
time	$\tau = \eta a_0/F_0$	
velocity	a_0/τ	$v \sim 5\mu m/s$
driving period	$T = 100\tau$	$T \sim 1.3$ s
viscosity coefficient	$\eta = F_0\tau/a_0$	$\eta \sim 10^{-3}$ Pa-s
substrate period	$\lambda = 1.825a_0$	$\lambda = 3.5\mu m$
substrate amplitude	$U_0 = 0.058E_0$	$U_0 = 75k_BT \sim 2J$
temperature	$T_0 = 0$ [a]	$T \sim 300K$

[a] to learn more about the effects of temperature on this simulation see Ex. IV D where we study the limit $U_0 \sim k_BT$.

III. MODE-LOCKING OF A SINGLE PARTICLE

A single particle responds to the applied driving force by moving across the landscape synchronized with the period of $F^d(t)$. The numerical implementation of the landscape is calculated with Eq. 1 as

$$F_y^l(y) = -A_p \sin(N_p \pi y/L) \tag{5}$$

where the force is scaled with parameter $A_p = N_p \pi U_0/L$. In this section, we fix the landscape parameters to $A_p = 0.1$ force units with $N_p = 20$ minima corresponding to a spatial period $\lambda = 1.825a_0$.

The driven particle adjusts its motion to traverse the periodic landscape with the same rhythm as the applied time-dependent force $F^d(t)$. When $F^d(t) > A_p$, a particle can overcome the barrier height of the landscape, and the particle hops between minima in the energy landscape. In Fig. 2(a) we plot $F^d(t)$ as a function of time with constants $F^{dc} = 0.1$, $F^{ac} = 0.05$ and $f = 0.01$ cycles per time unit τ. The temporal period of the driving force is $T = 1/f = 100\tau$. We mark the maxima of $F^{ac}(t)$ with the vertical dashed lines – i.e. $\sin(\omega t) = 1$. In Fig. 2(b) we show the $y-$position of the particle as a function of time. We normalize y by λ to show particle motion between substrate minima. The initial particle position is $y = 0$. As the driving force increases, the motion of the particle synchronizes with the driving period T. We measure average particle velocity $\langle v_y \rangle$ as the average displacement over the period of the driving force. The particle moves in the positive y-direction through $\Delta y = 2\lambda$ over the time period T, with the average velocity $\langle v_y \rangle = 2\lambda f$. The horizontal dashed lines coincide with minimum substrate force $F^l = -A_p$, i.e. $\sin(\pi y/\lambda) = 1$. The particle synchronizes its motion such that the driving force is maximum when the landscape force is minimum, as indicated with with the intersection of horizontal and vertical lines and the particle position y. The slope of y/λ is proportional to the net force on the particle. This can be seen in Fig. 2 where local extrema appear in y/λ when $F_D(t) \approx 0$.

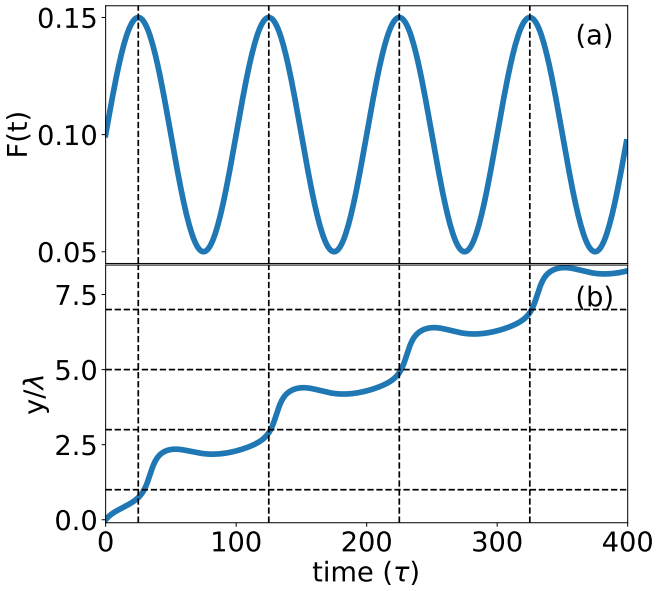

FIG. 2: (a) The applied driving force $F^d(t)$. (b) The $y-$position of the driven particle normalized by the period of the substrate λ.

The competition between the driving force and landscape potential can produce a variety of hopping patterns in the particle motion. The relative values of F^{ac}, F^{dc} and A_p control the rate and distance a particle moves forward and backward in the landscape. To explore the possible hopping patterns, we sweep through a range of F^{dc} for fixed F^{ac} and A_p to illustrate distinct oscillation modes. A mode is a periodic pattern of hops with a constant average particle velocity, $\langle v_y \rangle$ over a range of driving forces F^{dc}. In Fig. 3 we keep F^{dc} constant for 10^5 simulation timesteps and measure the average velocity $\langle v_y \rangle$ as a function of F^{dc}, with $F^{ac} = 0.05$, $f = 0.01$, and the landscape shown in Fig. 2. The modes appear as discrete steps in $\langle v_y \rangle$ across a range of F^{dc},

Each step represents a different pattern of hops between substrate minima performed by the particle due to the landscape confinement. In Fig. 3 at low F^{dc} the average velocity $\langle v_y \rangle$ is zero. Since A_p is large compared to the extrema of $F^d(t)$, the particle oscillates back and forth in a single minima with no net velocity. At higher F^{dc} the particle velocity $\langle v_y \rangle$ increases in steps of uniform height, $\langle v_y \rangle = n\lambda f$, where n is an integer. The step width is non-linear and can have a variety of interesting patterns such as a devil's staircase related to chaotic dynamics [12].

We explore a range of parameters in Ex. IV E where we perform this sweep for several values of F^{ac} including the limiting case that the applied force is a constant value.

When $F^{ac} = 0$, no steps appear in the $\langle v_y \rangle$ vs F^{dc} curve. When $F^{dc} - F^{ac} < -A_p$ the particle moves in the negative y-direction during part of the cycle. The period of the substrate can be used to control the intrinsic velocity of the dc driven particle, and the applied ac drive can cause mode-locking which appears as non-linear steps in the force-velocity relationship.

In the following section we include exercises to explore our numerical model, including the to linear drag equation in Ex. IV A, the equation of motion in Ex. IV B, and numerical integration techniques in Ex. IV C. An extended model that includes finite temperature effects is in Ex. IV D. We explore changes in the particle motion with parameter changes in Ex. IV E. Methods to visualize the dynamics of the particle motion are in Ex. IV F.

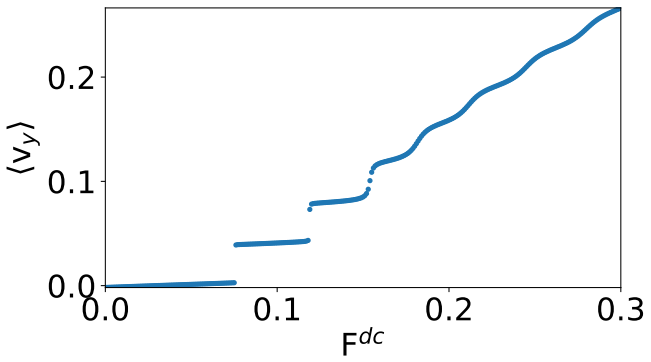

FIG. 3: Average particle velocity $\langle v_y \rangle$ as a function of F^{dc}, the constant parameter of $F^d(t)$ defined in Eq. 2. The remaining parameters in $F^d(t)$ are as in Fig. 2, $F^{ac} = 0.05$ and $f = 0.01$. [*I believe the slight slope in this curve is due to sampling - where does the particle start/end ?*]

IV. ASSOCIATED PROBLEMS

A. Drag Models and Reynolds Numbers.

Stokes' law describes the viscous drag on a sphere moving at velocity $\vec{v}$ as $\vec{F}^{lin} = -3\pi\eta D\vec{v}$ where η is the dynamic fluid viscosity and D is the particle diameter [37]. In simulation we subsume the constants $3\pi D$ such that $3\pi D\eta \to \eta$. Often drag forces are modeled as a polynomial series [37]

$$\vec{F}^{drag} = -b\vec{v} - cv^2\hat{v} + \dots . \tag{6}$$

Truncating the series to the first term is justified by demonstrating the sphere has a low Reynolds number $R = Dv\rho/\eta$ where ρ is the fluid density and v the particle's speed. When R is small, the quadratic and higher order terms may be ignored in favor of the linear drag term.

Using reasonable values for the experimental analog of this system, demonstrate the Reynolds number is low. In addition to the values listed in Table I, the liquid density ρ varies with temperature with $\rho \sim 10^3$ kg/cm^3 a reasonable first order approximation [40].

B. Equation of Motion

Newton's second law states that the acceleration of a particle i is proportional to the sum of forces on the particle

$$m_i\vec{a}_i = \sum \vec{F}_i \tag{7}$$

where the constant of proportionality is the inertial mass m_i. The addition of a dissipative force to a dynamical equation of colloid motion is typically modeled with a drag force proportional to the particle's velocity in the opposite direction of motion $\vec{F}^{drag} = -\gamma\vec{v}_i$ where $\gamma = 3\pi\eta D$ is the drag coefficient described in Ex. IV A. The ratio of m/γ is known as the momentum relaxation time, and is small for particles with low Reynolds numbers. The mass of the typical experimental colloid particle is 15 picograms, leading to a momentum relaxation time on the order of microseconds. Confirm for the values listed in Table I, the momentum relaxation time is $m/\gamma = 0.5$ μs.

When m/γ is small, particle acceleration can be ignored entirely. (a) Using Newton's Second Law for a small momentum relaxation time, demonstrate that a particle confined to a landscape exerting force $F^l(\vec{r}_i)$ subject to a time dependent drive $F^d(t)$ can be modeled with the equation of motion described in Eq. 3.

C. Integration Methods

To calculate the position of the particle we integrate the equation of motion using the standard definition of velocity $\vec{v}_i = d\vec{r}_i/dt$ via the Euler method. Our equation of motion provides a direct calculation for particle velocity, as demonstrated in Ex. IV B.

When solving ordinary differential equations, the Euler method is effective for solving linear equations of the form $dy/dt = f(t, y(t))$ with initial condition $y(t_0) = y_0$. The solution is calculated algorithmically by stepping in time through n integer steps $t_n = t_0 + n\Delta t$. At each subsequent step the new value for y is calculated as a map solution using discrete times $y_{n+1} = y_n + f(t_n, y_n)$. The Euler method can be applied to non-linear equations effectively if the time step Δt is kept sufficiently small [38]. In our simulations we use the timestep $\Delta t = 0.001$, but we find for a single particle we can just as easily used timesteps $\Delta t = 0.01$ and $\Delta t = 0.1$ over the same maximum time (i.e. decrease the overall simulation time and sampling rate) and reproduce the motions shown in Fig. 2(b). This is due to the linear nature of the solution,

and the lack of interaction with neighboring particles. Apply the Euler method to our equation of motion to solve for the analytic expression of position of a particle y_n at the *nth* timestep (i.e. Eq. 4).

small timesteps matter a great deal when particle interactions are included in the model. I have demonstrated that without particle interactions we can increase the timestep with no penalty, so this isn't a very interesting problem.

Often molecular dynamics algorithms are solved with higher order methods such as the Verlet method or Runge-Kutta methods. These methods include higher order terms that provide accurate solutions for second order differential equations, i.e. $dy/dt = v$ and $dv/dt = f_2(y,t)$. In Newton's second law f_2 would be proportional to the net force on a single particle.

In our model we do not integrate $f_2(y,t)$ since $a = dv/dt = 0$, and thus rearrange $f_2(y,t)$ to solve directly for v, as described in Ex. IV B. The Taylor expansion of the position function $y(t)$

$$y(t_n \pm \Delta t) = y(t_n) \pm \frac{dy}{dt}\Delta t + \frac{1}{2}\frac{d^2y}{dt^2}(\Delta t)^2 + \dots \quad (8)$$

is exact at first order for the n-th time step.

Demonstrate how the Verlet method simplifies to the Euler method when the particle acceleration $a = 0$.

D. Brownian motion

Brownian motion is a temperature and viscosity dependent phenomena in which particles change direction due to collisions with fluid particles. The frequency of collisions depends on the properties of the suspending fluid. These collisions are more likely at higher temperature due to the increased kinetic energy of the fluid particles, as described by the Maxwell-Boltzmann distribution [41].

In molecular dynamics simulations temperature effects can be modeled by including randomized forces f^T to emulate the motion of particles undergoing Brownian motion. A distribution of random forces contributes equally in all directions such that the force averaged over a finite time interval is zero $\langle f^T(t)\rangle = 0$. Random distributions are not correlated over the independent variable, where we take our independent variable to be time $\langle f^T(t) f^T(\tau)\rangle = 2\eta k_B T \delta(t-\tau)$ for a system with energy $k_B T$ derived from the Boltzmann constant k_B and temperature T [36]. A particle with energy $k_b T_{min} > U_0$ may hop over landscape barriers.

In simulation we define our temperature parameter to $k_b T/E_0 \rightarrow T$ since we set the constants to unity. In these units we can compare simulation temperature directly to force in order to estimate the degree of random fluctuation. For instance, with no applied driving force, the minimum temperature required for a single particle to hop between minima in the potential landscape is $T_{min} > A_p$. Assuming a particle is confined to move along the $y-$direction, include Brownian motion in the model, we find the crossover to a hopping regime at $T/A_p \approx 5.6$. We demonstrate this hopping pattern in a non-driven colloid for $T/A_p = 4.0, 5.0, 6.0$. Reproduce these results.

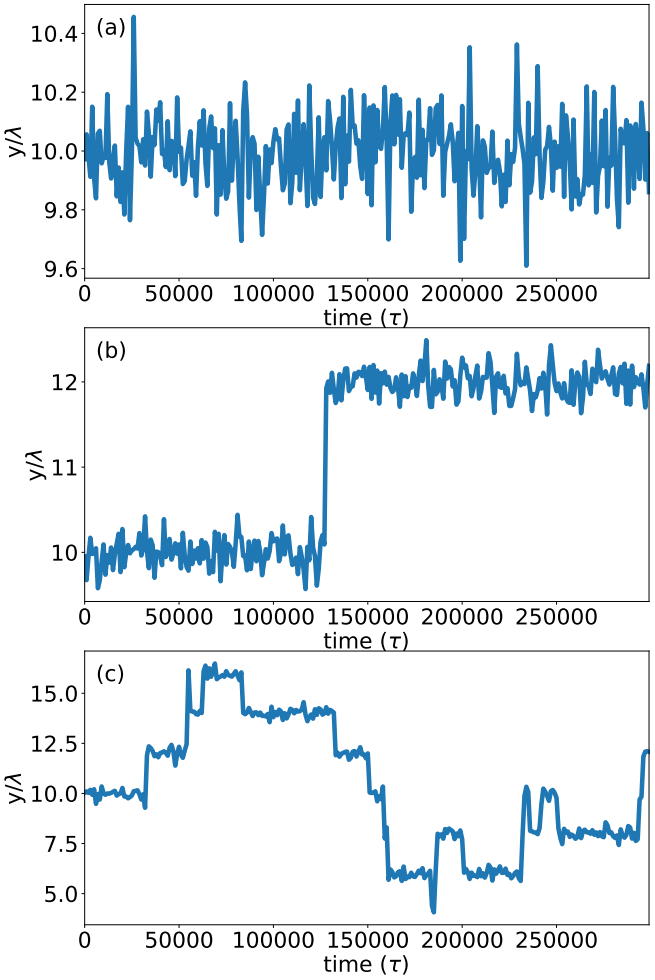

FIG. 4: Motion of a particle undergoing Brownian motion on a washboard potential energy landscape. (a) $T/A_p = 4.0$ no hopping occurs. (b) $T/A_p = 5.0$ a single hop occurs at $t = 130000$ (c) $T/A_p = 6.0$ many hops occur. Note the scale of the $y-$axis differs in each panel.

In Fig. 4 we show the position versus time of a simple particle confined to a sinusoidal landscape undergoing Brownian motion. We increase the temperature relative to the amplitude of the landscape troughs until the particle enters a hopping regime. In Fig. 4(a) $T/A_p = 4.0$ and the particle executes a random walk centered at the potential minima $y/\lambda = 10$. We ran many simulations and never observed a hop to another minima. In Fig. 4(b) $T/A_p = 5.0$ where hops between potential minima are possible but not probable, a single hop occurs from $y/\lambda = 10$ to $y/\lambda = 11$ at $t \sim 13000\tau$. In other simulations with identical parameters, we sometimes observed

no hops or two hops between minima, as expected with random fluctuating systems. In Fig. 4(c) $T/A_p = 6.0$ we observe approximately 15 hops, indicating the random thermalized kicks are sufficiently large to make the particle perform a random walk of hops a top the substrate in addition to the small scale random walk executed by all particles in this section.

A quantity of interest for a particle undergoing Brownian motion is the rate of displacement of the particle from its initial position This is measured as mean square displacement as a function of time

$$\langle \Delta\vec{r}(t)^2 \rangle = \langle (\vec{r}(t+t_0) - \vec{r}(t_0))^2 \rangle \tag{9}$$

where t_0 is the initial time at initial position $\vec{r}(t_0)$. With no substrate, we would expect the root mean square displacement (RMSD) to be proportional to the elapsed time

$$\sqrt{\langle \Delta\vec{r}(t)^2 \rangle} \propto t. \tag{10}$$

Confirm this result for $A_p = 0$. Measure the RMSD as a function of time of a non-driven colloid for $T/A_p = 0.5, 1.0$, and 2.0. Compare your result to the substrate free RMSD.

How does Brownian motion affect the formation of Shapiro steps? With driving force reproduce the paper figures...

E. Exploring Parameters of the Model

La la la...

F. Visualizing motion + phase plots

Drawing the contour

The code for generating a two dimensional colored plot of the potential landscape is calculated by evaluating the analytic function in Eq. 1 for a grid of values (x_n, y_n).

I have python code that does all of this, but I don't have it set up to play nice with my new python MD code

Also the animation library in python...

Phase plots...

V. CONCLUSION

A single particle oscillator in a potential well is much like a skateboarder in a half-pipe or a child on a swing. If subject to an applied force, a confined oscillator may synchronize its location to the periodic pattern of the external drive, moving back and forth in time with the beat. We have used a single particle driven across a periodic potential landscape to study synchronization dynamics that arise due to the interplay between a particles environment and external forces. The relationship between the driving force and landscape can change the pattern of motion. With a constant or dc drive the landscape modulates the particle velocity, below some threshold the dc force is not strong enough to push the particle across a potential maximum so the average velocity is zero, a phenomena referred to as pinning [23]. A sinusoidal or ac drive creates mode-locking, where the average particle velocity is fixed for a range of dc drive forces [24].

Our simulations reproduce results presented in Juniper *et al.* [25, 26] which demonstrated mode locking in experiments and simulations of driven colloids on a optical periodic landscape. Due to the relative ease of manipulation and imagining, colloids are used as experimental models for systems relatively hard to access and visualize. Collections of colloids can be used to study the properties of solids and liquids or more exotic systems such as cold atoms or electron gases [29]. Dynamical mode-locking, the primary synchronization effect explored in this paper, is observed in quantum electronic devices such as Josephson junctions [16, 17]. A single junction contains two superconductoring layers which sandwich an insulating layer. When subject to an external voltage, Cooper pairs in the superconducting materials tunnel through the insulating layer. Phase-locking is observed as stepped regions in current-voltage (I-V) relationship in these devices, where voltage is the analog of external driving force and current is that of particle velocity. Known as Shapiro steps, these phase locked currents have been observed due to applied ac voltages in single Josephson junctions [19, 21] and coupled arrays of junctions [20]. Shapiro steps vary in width depending on the strength of the applied ac forces, and are observed in a variety of systems displaying non-Ohmic behavior in voltage-current curves, including ac and dc driven charge and spin density waves and superconducting vortices in landscapes engineered with periodic patterns of pinning sites. Thus the study of mode-locking is a useful problem of complex quantum mechanical systems. Our results can be relevant to synchronization effects in a broad range of experiments systems including optically confined colloids, superconductors with periodic pinning arrays, and the charge and spin of atomic systems.

Acknowledgments

We acknowledge Harvey Gould and Jan Tobochnik, who invited us to write the article and supported its development. Charles and Cynthia Reichhardt advised the project and provided the original molecular dynamics code written in the C programming language. We acknowledge funding from the M.J. Murdock Charitable Trust and the Pacific Research Institute for Science and Mathematics.

[1] A. Pikovsky, M. Rosenblum, and J. Kurths, *Synchronization: A Universal Concept in Nonlinear Sciences* (Cambridge Univ. Press, Cambridge, 2003).

[2] M. Bennett, M.F. Schatz, H. Rockwood, and K. Wiesenfeld, Huygens' clocks, Proc. Roy. Soc. A **458**, 563 (2002).

[3] K. Okamoto, A. Kijima, Y. Umeno, and H. Shima. Synchronization in flickering of three-coupled candle flames. Sci Rep **6**, 36145 (2016)

[4] T. Arane, A. K. R. Musalem and M. Fridman, Coupling between two singing wineglasses, Am. J. Phys. **77**, 1066 (2009).

[5] J. Jia, Z. Song, W. Liu, J. Kurths, and Xiao, J. Experimental study of the triplet synchronization of coupled nonidentical mechanical metronomes. Sci. Rep. **5**, 17008 (2015).

[6] S. Portugal, T. Hubel, J. Fritz, S. Heese, D. Trobe, B. Voelkl, S. Hailes, A. M. Wilson and J. R. Usherwood. Upwash exploitation and downwash avoidance by flap phasing in ibis formation flight. Nature **505**, 399 (2014).

[7] I. Aihara, T. Mizumoto, T. Otsuka, H. Awano, K. Nagira, H. G. Okuno and K. Aihara. Spatio-Temporal Dynamics in Collective Frog Choruses Examined by Mathematical Modeling and Field Observations. Sci Rep **4**, 3891 (2014).

[8] P. Tranchant, D. T. Vuvan, and I. Peretz, Keeping the Beat: A Large Sample Study of Bouncing and Clapping to Music. PLoS ONE 11(7): e0160178. (2016).

[9] G. Martin Hall, Sonya Bahar, and Daniel J. Gauthier, Prevalence of Rate-Dependent Behaviors in Cardiac Muscle. Phys. Rev. Lett. **82**, 2995 (1999).

[10] W. Singer. Striving for coherence. Nature, **397** 391, 1999.

[11] Dutta, S., Parihar, A., Khanna, A. et al. Programmable coupled oscillators for synchronized locomotion. Nat Commun **10**, 3299 (2019).

[12] P. Bak. The Devil's Staircase. Physics Today **39**, 12, 38 (1986).

[13] J. A. Lissajous. "Mmoire sur l'Etude optique des mouvements vibratoires," Annales de chimie et de physique, 3rd series, 51 (1857) 147-232

[14] E. Y. C. Tong, Lissajous figures, The Physics Teacher **35**, 491 (1997).

[15] E. M. Purcell, Life at low Reynolds numbers, Am. J. Phys. **45**, 311 (1977).

[16] B. D. Josephson, Phys. Letters **16**, 25 (1962).

[17] B. D. Josephson, Advan. Phys. **14**, 419 (1965).

[18] W. C. Stewart CurrentVoltage Characteristics of Josephson Junctions, Appl. Phys. Lett. 12, 277 (1968).

[19] S. Shapiro, Josephson currents in superconducting tunneling: the effect of microwaves and other observations, Phys. Rev. Lett. 11, 80 (1963).

[20] S. P. Benz, M. S. Rzchowski, M. Tinkham, and C. J. Lobb, Fractional giant Shapiro steps and spatially correlated phase motion in 2D Josephson arrays, Phys. Rev. Lett. 64, 693 (1990); D. Domnguez and J. V. Jose, Giant Shapiro steps with screening currents, Phys. Rev. Lett. 69, 514 (1992).

[21] A. A. Golubov, M. Yu. Kupriyanov, and E. Ilichev. The current-phase relation in Josephson junctions, Rev. Mod. Phys. **76**, 411 (2004).
quote: Phase engineering techniques are used to control the dynamics of long-bosonic Josephson-junction arrays built by linearly coupling Bose-Einstein condensates.

[22] Dengling Zhang, Haibo Qiu, and Antonio Muoz Mateo, Unlocked-relative-phase states in arrays of Bose-Einstein condensates, Phys. Rev. A **101**, 063623 (2020).

[23] C. Reichhardt and C. J. Olson Reichhardt, Depinning and nonequilibrium dynamic phases of particle assemblies driven over random and ordered substrates: a review, Rep. Prog. Phys. 80, 026501 (2017).

[24] C. Reichhardt, and C. J. O. Reichhardt, Shapiro steps for skyrmion motion on a washboard potential with longitudinal and transverse ac drives. Phys. Rev. B **92**, (22). (2015).

[25] M. P. N. Juniper, A. V. Straube, R. Besseling, D. G. A. L. Aarts, and R. P. A. Dullens, Microscopic dynamics of synchronization in driven colloids. Nat. Commun. 6, 7187 (2015).

[26] Juniper, M. P. N., Zimmermann, U., Straube, A. V., Besseling, R., Aarts, D. G. A. L., Lwen, H., and Dullens, R. P. A. Dynamic mode locking in a driven colloidal system: Experiments and theory. New Journal of Physics, 19(1). (2017).

[27] S. Herrera-Velarde and R. Castaeda-Priego, Superparamagnetic colloids confined in narrow corrugated substrates, Phys. Rev. E **77**, 041407 (2008).

[28] S. Herrera-Velarde and R. Castaeda-Priego, J. Phys.: Condens. Matter 19, 226215 (2007).

[29] D. G. Grier, A revolution in optical manipulation. Nature **424**, 810 (2003).

[30] Arthur Ashkin, Optical trapping and manipulation of neutral particles using lasers, Proc. Natl. Acad. Sci. U.S.A. 94, 48534860 (1997).

[31] G. Volpe and G. Volpe, Simulation of a Brownian particle in an optical trap, Am. J. Phys. 81 (3), March 2013

[32] C. Lutz, M. Kollmann, and C. Bechinger, Phys. Rev. Lett. **93**, 026001 (2004); C. Lutz, M. Kollmann, C. Bechinger, and P. Leiderer, J. Phys.: Condens. Matter **16**, S4075 (2004).

[33] S. Tarucha, T. Honda, T. Saku, Solid State Commun. 1995, 94, 413.

[34] A. Gholami, O. Steinbock, V. Zykov, and E. Bodenschatz, Flow-Driven Waves and Phase-Locked Self-Organization in Quasi-One-Dimensional Colonies of Dictyostelium discoideum, Phys. Rev. Lett. **114**, 018103 (2015).

[35] D. Frenkel and B. Smit, Understanding Molecular Simulation: From Algorithms to Applications (Academic Press, London, 2001).

[36] M. P. Allen and D. J. Tildesley, Computer Simulation of Liquids. Second Edition. Oxford University Press (2017).

[37] J. Taylor, Classical mechanics. University Science Books (2005).

[38] M. Newman, Computational Physics, CreateSpace Independent Publishing Platform. (2012).

[39] Supplementary videos coming soon.

[40] IAPWS R12-08, Release on the IAPWS Formulation 2008 for the Viscosity of Ordinary Water Substance, September 2008, http://www.iapws.org/relguide/viscosity.html

[41] A Einstein, Investigations on the Theory of the Brownian Movement, Dover Publications (1956).